

Article

A “Status-Habitat-Potential” Model for the Evaluation of Plant Communities in Underwater Mining Areas via Time Series Remote Sensing Images and GEE

Jiixin Mi ^{1,*}, Deli Yang ^{1,2,*}, Huping Hou ¹ and Shaoliang Zhang ^{2,3} 

¹ School of Public Policy and Management, China University of Mining and Technology, Xuzhou 221008, China; houhuping@cumt.edu.cn

² Office of Undergraduate Academic Affairs, China University of Mining and Technology, Xuzhou 221008, China; slzhang@cumt.edu.cn

³ School of Environment Science and Spatial Informatics, China University of Mining and Technology, Xuzhou 221008, China

* Correspondence: jxmi@cumt.edu.cn (J.M.); yangdl@cumt.edu.cn (D.Y.)

Abstract: Mining activities are the primary human-induced disturbances on plant communities in various ecosystems, and they also are important for implementing strategies of ecological protection and restoration based on them. The effects of underwater mining on plant communities in wetland ecosystems, however, are seldom demonstrated, and it is also difficult to accurately evaluate the state of plant communities' condition, considering the dynamic and randomness of plant communities under multiple factors, including climate, mining, and other human activities. To address these issues, a “Status-Habitat-Potential” (SHP) model has been developed, with nine indicators from the status, habitat, and potential of plant communities, and the plant communities in the Nansi Lake mining area are evaluated to illustrate the effects of underwater mining. Time series remote sensing images from Sentinel-2 and Google Earth Engine are applied. Comparison analysis, Global Moran's index, and hot and cold analysis are also used to demonstrate the spatial characteristics of the SHP index. Results show that the SHP index varies between 0 and 0.57 and shows a high aggregation pattern according to the Global Moran's index (0.41), with high and low values aggregating in the center of the lake and living areas, respectively. The SHP index between subsidence and contrast areas shows no significant difference (at $p < 0.05$), indicating little effect of mining subsidence on plant communities directly. Overall, underwater mining would not cause as obvious effects on plant communities as underground mining, but human activities accompanied by mining activities will result in the loss of plant communities around lake shores and river channels. This study put forward a new model to evaluate plant communities in terms of their status, habitat, and potential, which could also be used to illustrate other long-term effects of disturbances on plant communities.

Keywords: underwater mining; subsidence; plant evaluation; time series remote sensing; Google Earth Engine



Citation: Mi, J.; Yang, D.; Hou, H.; Zhang, S. A “Status-Habitat-Potential” Model for the Evaluation of Plant Communities in Underwater Mining Areas via Time Series Remote Sensing Images and GEE. *Land* **2023**, *12*, 2097. <https://doi.org/10.3390/land12122097>

Academic Editors: Xinxin Wang, Yongchao Liu, Jie Wang and Xiaocui Wu

Received: 31 October 2023

Revised: 15 November 2023

Accepted: 21 November 2023

Published: 22 November 2023



Copyright: © 2023 by the authors. Licensee MDPI, Basel, Switzerland. This article is an open access article distributed under the terms and conditions of the Creative Commons Attribution (CC BY) license (<https://creativecommons.org/licenses/by/4.0/>).

1. Introduction

Conflicts between coal mining and ecological conservation have become a significant factor that constrains the sustainable development of mining areas. In underground mining areas, coal mining has caused serious impacts on surface ecosystems [1–4], especially on plant communities, often resulting in deaths or damage to plants [5], and degradation of plant communities [6]. Evaluating plant communities and quantifying the effects of mining have become important parts of ecological protection and restoration in mining areas [7]. Among all underground mining areas, underwater mining is a special type, because the surface hazards caused by underwater mining are often overlooked due to being covered by water, and the impact of underwater mining on plant communities is ignored as well.

To develop appropriate strategies and management measures for ecological conservation, it is necessary to evaluate plant communities under the disturbance of underwater mining.

The impacts of underwater mining on wetland plant communities have been a subject of controversy. It is widely believed that waterlogging areas formed by underground mining in high groundwater areas provide new habitats and abundant water sources, thus promoting the development of plant communities [8,9]. Similarly, some studies suggest that subsidence caused by underwater mining increases the depth and capacity of water [10,11], which would also benefit wetland plants [12]. Additionally, subsidence may also create diverse habitats, which favors the increase in species diversity [11]. On the contrary, some studies argued that changes in the water depth can affect the development of existing plant communities [13–15]. For example, increased water depth may result in the loss of living space for some emergent plants and limit their survival [16]. Ground cracks associated with subsidence can lead to water resource loss [17,18], causing the mined wetlands to remain drier with shorter water retention times and less spatial variation compared to undisturbed wetlands. Overall, there are still differing opinions on the effects of underwater coal mining on plant communities, which undoubtedly leads to difficulties in developing wetland ecological conservation policies.

Unstable dynamic changes in wetland plant communities are responsible for the divergence of opinions on the impacts of underwater mining. Wetland plant communities are influenced by various climatic factors such as rainfall and temperature [19,20], showing fluctuations in water levels between different years [21], which can cause changes in the coverage, type, and density of plant communities [22–24], and thus, wetland ecosystems exhibit randomness and volatility in the changes in plant communities [25,26]. Moreover, based on the disturbance characteristics of underground mining, the disturbance process may persist for 1–2 years [27], while plant growth and changes in communities are also long-term and slow processes [28]. However, previous studies mostly reflected the influences on plant communities through changes observed between different years [29–31], making it difficult to objectively and accurately reflect the dense dynamic of wetland plant communities. To reveal the impact of underground coal mining on plant communities, it is necessary to develop new methods for quantitatively evaluating wetland plant communities.

The goal of this study was to develop a new model for the evaluation of plant communities in underwater mining areas and to illustrate the impacts of underwater mining on wetland plant communities. The Nansi Lake, China was selected as the study area. The main objectives of this research were to (1) propose a quantitative model to evaluate plant communities in underwater mining areas while considering the fluctuation of plant communities under the driving effects of natural force, and (2) illustrate the impacts of underwater mining on wetland plant communities in the Nansi Lake.

2. Materials and Methods

2.1. Study Area

Nansihu Wetland (116°34′–117°24′ E, 34°27′–35°20′ N) is located in the northern part of the Huai River Basin in East China. It is the sixth largest freshwater lake in China and the most important natural reservoir in Shandong Province (Figure 1). The lake covers an area of 1289 km² and serves as an important water supply channel, as well as a reservoir for the South-to-North Water Transfer Project. Apart from the Beijing and Hangzhou channels, the average depth of the lake is close to 1.5 m. Its capacity is approximately 6.37×10^9 m³, receiving drainage from 54 rivers. During flood periods, the lake becomes a shallow, open-plain grassland lake. The water flows from north to south and eventually merges with the ocean through the Huai River. The lake falls within the warm temperate monsoon climate zone, with an average annual temperature of 13.7 °C. The average annual rainfall ranges from 550 to 720 mm, with nearly 60% concentrated in the rainy summer months. The average annual natural runoff is 2.96×10^{10} m³.

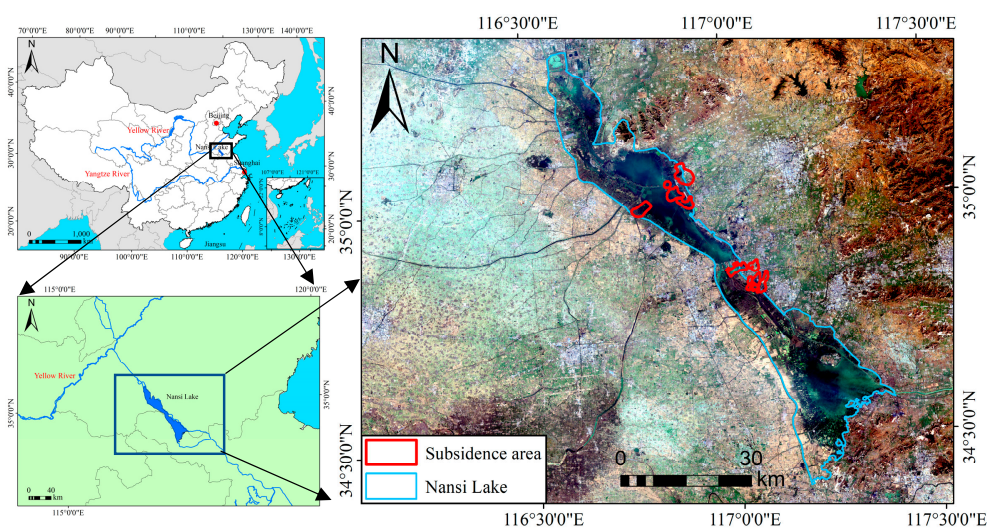


Figure 1. Locations of Nansi Lake and subsidence area.

There are seven coal mines currently being mined under Nansihu Lake. The average total thickness of the coal seams is 5.78 m, accounting for 82% of the total thickness of economically viable coal seams. The coal quality is medium grade. Fully mechanized caving longwall mining and thin coal seam comprehensive mechanized mining technologies are employed. The mining depth ranges from -90 m to -1500 m in multiple coal seams. The annual production capacity is 12 million tons. By 2020, a total of 61.6 km² subsidence was caused by mining activities (Figure 1).

2.2. “Status-Habitat-Potential” Model for Plant Communities

A quantitative model for evaluation of plant communities in wetland ecosystems from the perspectives of the status, habitat, and potential are developed in this research. The status of plant communities, which can be represented by various plant indicators and remote sensing indices, such as plant coverage, richness, and density, as well as normalized difference vegetation index (NDVI), is able to reflect the structure and function of the community. The habitat where plant communities are located is equally significant to them, including factors such as soil, topography, and hydrology, which can be demonstrated by soil organic matter, slopes, and water content, as well as some remote sensing indices, such as normalized difference water index (NDWI). The elements of habitat determine whether a plant community has a stable growing environment and sufficient access to energy, nutrients, and water, during growth and succession processes. The potential of plant communities is important in indicating their development in the future and is often related to the resilience, resistance, and stability of the plant communities, which should also be considered in evaluation and can be assessed based on previous changes in plant communities. Therefore, a “Status-Habitat-Potential” model for plant communities, including nine indicators, is put forward, as shown in Figure 2, to make a comprehensive evaluation of underwater mining areas.

Considering the spatial and temporal characteristics of plant communities, as well as their habitats in wetland ecosystems, NDVI and NDWI were selected as the basic parameters of plant communities and habitats. Because the effects of climate, phenology, and underwater mining on plant communities could vary over a long period of time, it would be inaccurate to evaluate plant communities by the NDVI or NDWI at a single time point. To address this issue, a total of nine indicators based on time series NDVI and NDWI revealing the status, habitat and potential of plant communities were selected: (1) plant types, (2) NDVI minimum, (3) NDVI maximum, (4) average NDWI, (5) variance of NDWI, (6) water coverage frequency, (7) variance of NDVI, (8) trend of NDVI and (9) Kendall’s tau-b coefficient. The definitions and equations of each indicator are shown as follows.

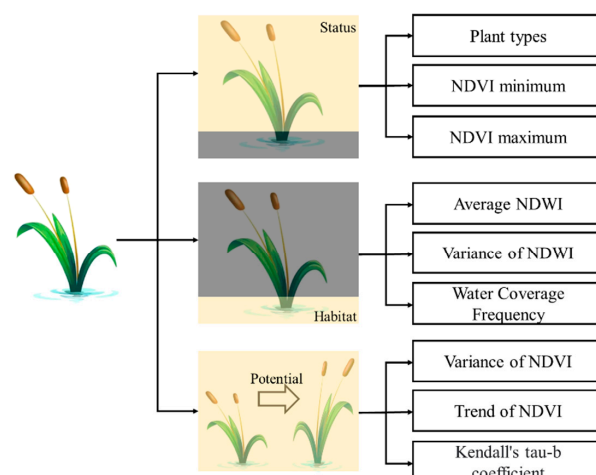


Figure 2. Framework of “Status-Habitat-Potential” model and indicators.

(1) Plant types

Plant types can reflect the hierarchy of communities and have certain indicative roles in predicting future changes, as well as the development of plant communities. This study selects 2020 as the targeted year, and ESA WorldCover 2020 is selected as the baseline data for plant types. ESA WorldCover 2020 is a global land cover map with a 10 m resolution based on Sentinel-1 and Sentinel-2 data in 2020, which includes 11 land cover categories, namely forest, shrubland, grassland, cropland, built-up areas, bare/sparse vegetation areas, snow and ice, water bodies, herbaceous wetlands, mangroves, and mosses/lichens. Each plant type is evaluated and scored for the calculation of SHP index.

(2) NDVI maximum

NDVI maximum is the average value of annual maximum NDVI ($NDVI_{max}$), reflecting the NDVI of vegetation when it is in the best growth conditions. NDVI maximum generally occurs in summer. For the same type of plant community, the larger NDVI maximum indicates that the community has a healthier state under the optimal environment; conversely, it indicates that the community has certain defects and is difficult to fully utilize nutrients. NDVI maximum is calculated by Equation (1):

$$NDVI_{max} = \frac{NDVI_{max}y_i}{n} \quad (1)$$

where $NDVI_{max}y_i$ is the maximum value of NDVI in year i , and n is the number of years in this study ($i = [1, 2, 3, 4, 5]$, $n = 5$).

(3) NDVI minimum

NDVI minimum is the average value of annual minimum NDVI ($NDVI_{min}$) and reflects the NDVI of vegetation when it is in the poorest growth conditions, which usually occurs in winter. For the same type of plant community, the larger the NDVI minimum, the stronger the tolerance to cold and drought; conversely, it indicates that the plant community finds it difficult to maintain stability under external disturbances. NDVI minimum is calculated by Equation (2):

$$NDVI_{min} = \frac{NDVI_{min}y_i}{n} \quad (2)$$

where $NDVI_{min}y_i$ is the minimum value of NDVI in year i , and n is the number of years in this study ($i = [1, 2, 3, 4, 5]$, $n = 5$).

(4) Average NDWI

The average NDWI reflects the average level of water resources in a wetland over a certain period of time. For wetland plant communities, a higher annual average NDWI

indicates that vegetation has sufficient water supply to meet its growth requirements. The average NDWI is calculated by Equation (3):

$$NDWI_{ave} = \frac{NDWI_j}{j} \quad (3)$$

where $NDWI_j$ is the value of NDVI in image j , and j is the number of images collected in this study ($j = 709$).

(5) Variance of NDWI

The variation of NDWI reflects the stability of water bodies in a certain period of time. Generally, stable water bodies tend to maintain similar levels of NDWI, and there is not much variation between different years. On the other hand, unstable water bodies often experience fluctuations in water level due to factors like rainfall. These fluctuations can limit the growth of aquatic plants and make it difficult for them to survive during dry seasons. The variance of NDWI is calculated by Equation (4):

$$NDWI_{variance} = \frac{NDWI_{std}}{NDWI_{mean}} \times 100\% \quad (4)$$

where $NDWI_{std}$ and $NDWI_{mean}$ are the standard deviation and mean value of NDWI in all images collected in this study.

(6) Water coverage frequency

Water coverage frequency is the frequency at which a certain area maintains water cover during multiple observations. Similar to NDWI, Water coverage frequency is also an indicator showing the stability of water body and is calculated by comparing the number of times that each pixel is identified as water in the remote sensing images to the total number of remote sensing images. The water coverage frequency is calculated by Equation (5):

$$WCF = \frac{n_{water}}{n_{image}} \times 100\% \quad (5)$$

where n_{water} and n_{image} are the numbers of each pixel being identified as water and remote sensing images, respectively.

(7) Variance in NDVI

The variation in NDVI can reflect the stability of plant communities facing external interference. A larger variance of NDVI implies more intense vegetation fluctuations, making it more susceptible to disturbances, and it can be considered that plant communities with stronger NDVI stability have greater development potential. The variance of NDVI is calculated by Equation (6):

$$NDVI_{variance} = \frac{NDVI_{std}}{NDVI_{mean}} \times 100\% \quad (6)$$

where $NDVI_{std}$ and $NDVI_{mean}$ are the standard deviation and mean value of NDVI in all images collected in this study.

(8) Trends in NDVI

Trends in NDVI reflect the overall change direction of plant communities in a certain period, which is an important phenological index in long-term assessment, and is estimated from the linear term of a regression on the full-time series of collected images in this study. In this study, the trend of NDVI is calculated directly by the function of “*formaTrend*” documented in GEE.

(9) Kendall’s tau-b rank correlation

Kendall's tau-b rank correlation coefficient is a measure of the degree of correlation between two ordered variables, applicable when both categorical variables are in an ordered category. The Kendall's tau-b correlation coefficient ranges from -1 to $+1$. A value less than 0 represents a negative correlation, greater than 0 represents a positive correlation, and equal to 0 indicates no correlation. The closer the correlation coefficient is to 0 , the weaker the correlation; the closer it is to -1 or $+1$, the stronger the correlation. For time series NDVI data, Kendall's tau-b rank correlation coefficient calculates the relationship between NDVI and its order, reflecting the trend of NDVI changes over time. This can be used to predict future changes based on the historical vegetation dynamics. In this study, functions built in the GEE platform calculating Kendall's tau-b rank correlation coefficient are directly applied to process and visualize the NDVI data in the study area.

Based on above nine indicators, a Status-Habitat-Potential (SHP) index is calculated by normalizing and weighting each indicator. The weights of each indicator are determined by the entropy method. The calculation steps of the weight by entropy methods are as follows.

(1) Calculate the proportion of the s^{th} value of the t^{th} indicator as follows:

$$p_{st} = \frac{x_{sy}}{\sum_{s=1}^n x_{st}} \cdot (s = 1, 2 \dots n, t = 1, 2 \dots m) \quad (7)$$

(2) Calculate the entropy of the t^{th} indicator:

$$e_t = -k \sum_{s=1}^n p_{st} \ln(p_{st}) \quad (8)$$

where $k > 0$ and is given by:

$$k = \frac{1}{\ln(n)} \quad (9)$$

(3) Calculate the coefficient of variance for the t^{th} indicator as follows:

$$d_t = 1 - e_j \quad (10)$$

(4) Calculate the weight as follows:

$$\omega_t = \frac{d_t}{\sum_{t=1}^m d_t} \quad (11)$$

where n and m represent the number of sample points, and the number of indicators, respectively.

2.3. Acquisition and Analysis of Time Series Remote Sensing Images with GEE

Time series remote sensing images are acquired and analyzed via Google Earth Engine (GEE) to calculate indicators of the SHP model, and the spatial characteristics of SHP index are further analyzed (Figure 3). In this study, Sentinel-2 images (Sentinel-2 MSI: MultiSpectral Instrument, Level-2A, ESA) of the study area within 2018 and 2022 are all selected through Google Earth Engine (GEE), which have 13 spectral bands: four bands at 10 m, six bands at 20 m and three bands at 60 m spatial resolution, as well as are atmospherically corrected as surface reflectance product. A total of 709 images were acquired in this study. After that, filtered images are preprocessed by clipping, mosaicking, and stacking to construct time series images, as well as adding the two new bands, NDVI and NDWI, into image collections on GEE (Supplementary Materials S1 and S2). A detailed method of pre-processing with Google Earth Engine Code Editor is provided in the supplement material. Then, various indicators are calculated and normalized based on the time series data. Next, the SHP index is computed with nine indicators and the entropy weighting method. Finally, a comparative analysis between subsidence and contrast areas is used to reflect the effect

of underwater mining on plant communities. To demonstrate the spatial characteristics of plant communities under effects of the underwater mining, spatial analysis was also performed with the distribution of SHP index via Global Moran’s index [32] and hot spot analysis [33]. Global Moran’s index is regarded as one of the most widely used methods to estimate spatial autocorrelation of each index, which can effectively characterize the clustering of whole region, and the positive values for Moran’s I suggest positive spatial autocorrelation, while negative values indicate spatial outliers. The function of Global Moran’s index is shown as follows:

$$I = \frac{n}{S_0} \times \frac{\sum_{i=1}^n \sum_{j=1}^n w_{ij} (y_i - \bar{y})(y_j - \bar{y})}{\sum_{i=1}^n (y_i - \bar{y})^2} \tag{12}$$

$$S_0 = \sum_{i=1}^n \sum_{j=1}^n w_{ij} \tag{13}$$

where n is the total number of samples; y_i and y_j represent SHP indices in the sample at location i and j , respectively; \bar{y} is the average value of SHP index in all samples; w_{ij} is the spatial weight between sample locations i and j .

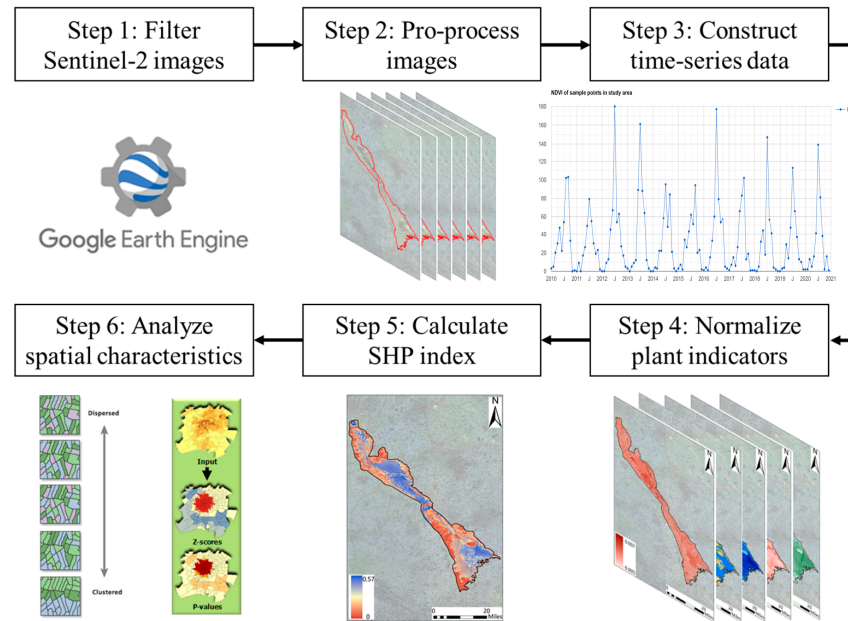


Figure 3. Flow chart of evaluation for plant communities via SHP model.

Hot spot analysis is a mapping technology that can reveal hidden spatial clusters based on the distance between samples, which can identify locations with statistically significant high and low values in a certain geographic area. Getis-Ord G_i^* statistic is a measure of spatial autocorrelation at the local scales, indicating high and low values that are associated with the hot spot and cold spot cluster patterns, respectively. The statistically significant hot spot is returned with high z-scores and small p -values. In contrast, the high negative z-scores and small p -values indicate significant cold spots. The function of Getis-Ord G_i^* statistic is shown as follows:

$$G_i^* = \frac{\sum_{j=1}^n w_{ij} x_j - \bar{X} \sum_{j=1}^n w_{ij}}{\sqrt{\frac{n \sum_{j=1}^n w_{ij}^2 - (\sum_{j=1}^n w_{ij})^2}{n-1}}} \tag{14}$$

where i is the center of the local neighborhood; x_j is the SHP index in the sample at location j ; w_{ij} is the spatial weight between sample locations i and j ; n is the total number of samples.

Due to the difference in dimensions, units, and meanings among SHP indicators, indicators should be normalized before calculating the SHP index. Each plant type is scored based on its significance in function to wetland ecosystems, and the scoring table is shown in Table 1. Tree cover, shrubland, and grassland are scored based on the hierarchy of plant community, with scores of 1, 0.8, and 0.6, respectively; herbaceous wetland, permanent water bodies, and bare/sparse vegetation, are scored according to the suitability for wetland vegetation, with scores of 0.8, 0.4, and 0.2, respectively; considering the intensive human activities on cropland and built-up, which make it difficult for wetland plants to survive, they are both scored with 0. For positively correlated indicators, including NDVI minimum, NDVI maximum, average NDWI, water coverage frequency, trend of NDVI, and Kendall's tau-b rank correlation, larger values indicate better plant community conditions and greater stability. Therefore, the normalization with maximum and minimum values is applied. As for negatively correlated indicators, including variances of NDVI and NDWI, larger values indicate greater fluctuation of plant communities, and thus, reciprocal processing is performed before normalization with maximum and minimum values. The normalized value of each indicator is calculated by Equation (12):

$$I_{normalization} = \frac{I_j}{I_{max} - I_{min}} \times 100\% \quad (15)$$

where I_j is the value of indicator j , and I_{max} and I_{min} are the maximum and minimum of indicator j among all images ($j = 9$).

Table 1. Scores for different types of land cover.

Types	Scores
Tree cover	1
Shrubland	0.8
Grassland	0.6
Cropland	0
Built-up	0
Bare/sparse vegetation	0.2
Permanent water bodies	0.4
Herbaceous wetland	0.8

2.4. Statistical and Spatial Analysis

Analysis of variance was performed to analyze the variation of SHP index between subsidence and contrast areas by random points selected within two areas. Significant differences between subsidence and contrast areas were evaluated at the 0.05 level with a Duncan test. All data were analyzed using SPSS 20.0 and MATLAB software R2023a; diagrams were made using Origin 9 software; Global Moran's index and hot spot analysis were calculated and performed in ArcMap 10.6 software.

3. Results

3.1. Status-Habitat-Potential Indicators of Plant Communities in Nansi Lake

The Status-Habitat-Potential indicators of plant communities in Nansi Lake are shown in Figure 4. In 2020, the plant communities in Nansi Lake consist of trees, shrubs, grass, and herbaceous wetland vegetation. The NDVI maximum ranges from -0.37 to 0.95 , while the low-value part is mainly located at built-up and bare land, and the highest value reaching 0.95 indicates that the regional vegetation is extremely lush, and mainly distributed around lakes. The NDVI minimum ranges from -0.95 to 0.03 . The low values of the NDVI minimum are mainly concentrated in land areas such as woodland, cultivated land, and grassland, while the high values are distributed around water bodies, indicating that the plant community in the study area is almost unable to survive in winter.

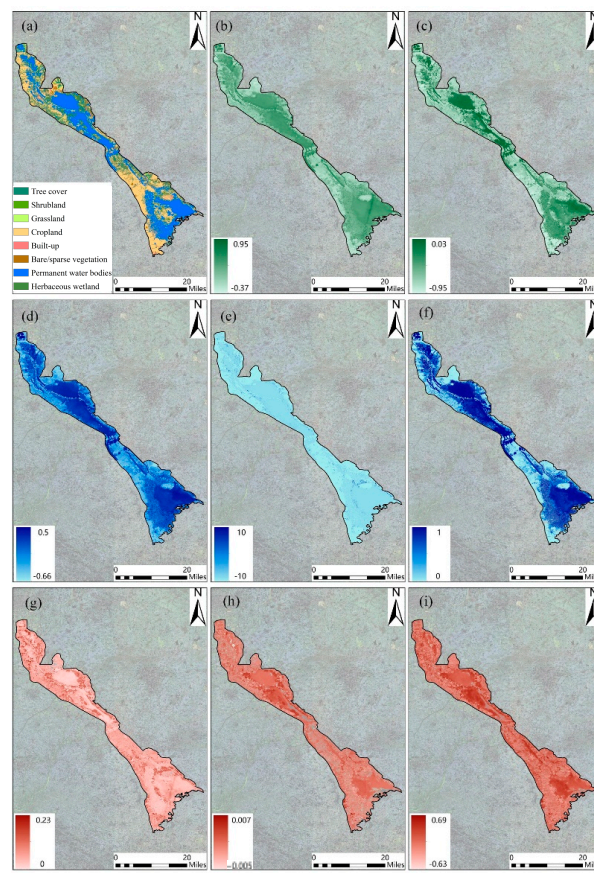


Figure 4. SHP indicators in Nansi Lake. (a) Plant types, (b) NDVI minimum, (c) NDVI maximum, (d) average NDWI, (e) variance of NDWI, (f) water coverage frequency, (g) variance of NDVI, (h) trends in NDVI and (i) Kendall's tau-b coefficient.

The average NDWI ranges from -0.66 to 0.5 , and the high-value areas are mainly water bodies and some plant-cover areas, while the low-value areas are those without water or plants such as built-up and bare land. The variance of NDWI varied between -10 and 10 , and the areas with large variation are generally those where land cover types changed, such as cultivated land transforming into water bodies, bare land transforming into water bodies, or the opposite type. In terms of water coverage frequency, the margins of Nansi Lake are obviously greater than the central part of the lake, indicating greater fluctuations in the habitats of plant communities.

The variation of NDVI is between 0 and 0.23 , compared with the NDWI variation, and it can be found that the changes in NDVI are relatively small. The high-value area of the NDVI variation is located at the junction of water and land, while the central part of the lake maintains a low variance in NDVI. The trend of NDVI ranges from -0.005 to 0.007 and the areas with positive values are mainly concentrated in the center of the lake, while the values in areas with dense human activities such as lakeshores are mostly negative. In addition, NDVI Kendall's tau-b rank correlation coefficient also reflects the changing trend of plant communities, with values ranging from -0.63 to 0.69 , which show a more obvious trend than NDVI variance because it only establishes a correlation rather than a quantitative relationship between time series and NDVI. Similarly, the central area of the lake shows a higher positive trend than the edge areas of Nansi Lake. Based on the original values of Status-Habitat-Potential indicators, the normalized values of each indicator are calculated, which will be further applied to estimate the SHP index with the entropy method.

3.2. Distribution and Spatial Characteristics of SHP Index in Nansi Lake

The distribution of the SHP index is shown in Figure 5, and the spatial characteristics of SHP indices are analyzed with Global Moran's index and hot spot analysis. The weights of the SHP indicators vary between 0.08–0.12, indicating a similar significance for each indicator (Table 2), and the SHP index is calculated according to the weights of each indicator. The SHP index of plant communities in Nansi Lake is between 0 and 0.57, with high-value areas concentrated in the central part of the lake, which is covered by water bodies, trees, and herbaceous wetlands in terms of land cover. Overall, the SHP index in Nansi Lake is generally at a medium level.

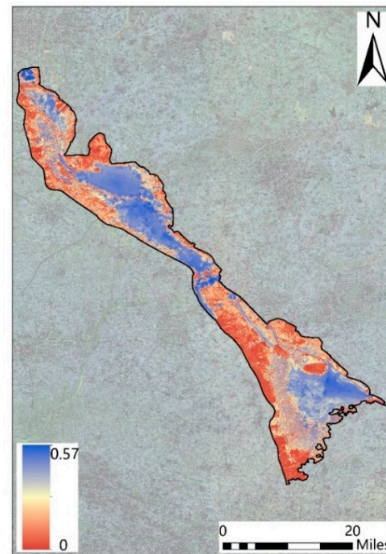


Figure 5. Spatial distribution of SHP index in Nansi Lake.

Table 2. Weights of SHP indicators in Nansi Lake.

Indicators	F1	F2	F3	F4	F5	F6	F7	F8	F9
Weights	0.12	0.11	0.08	0.11	0.12	0.11	0.12	0.12	0.12

F1: plant types, F2: NDVI maximum, F3, NDVI minimum, F4, average NDWI, F5, variance of NDWI, F6, water coverage frequency, F7: variance of NDVI, F8: trend of NDVI and F9: Kendall's tau-b coefficient.

The spatial characteristics of SHP indices are analyzed with Global Moran's index (Table 3) and hot spot analysis. From the perspective of spatial distribution, the Global Moran's index is 0.41, with z score equaling 456.32 and p equaling 0, indicating an aggregated pattern in Nansi Lake. Furthermore, the hot and cold spots are analyzed and distributed as shown in Figure 6. The high values of the SHP index mostly aggregate in the central part of the lake, while the low values of the SHP index mainly aggregate in areas that are cropland and built up, and the SHP index in other areas is not randomly distributed.

Table 3. Global Moran's index test results.

Indices	Values
Global Moran's I	0.41
z score	456.32
p	0

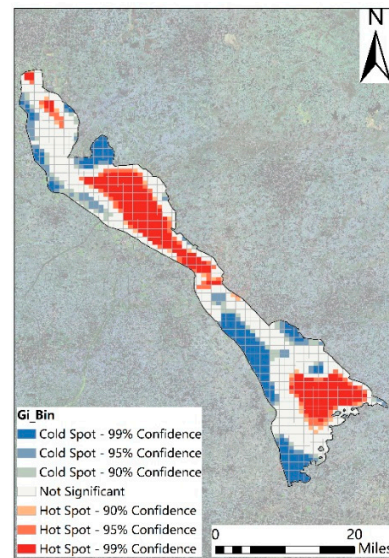


Figure 6. Cold and hot spots of SHP index in Nansi Lake.

3.3. Comparison of SHP Index between Subsidence and Contrast Areas

Differences in the SHP index of plant communities between the subsidence and contrast areas in Nansi Lake are demonstrated by comparing the values of random sample points within two areas. Based on the spatial distribution map of mining subsidence obtained from local mine enterprises, Nansi Lake is divided into subsidence and contrast areas, as shown in Figure 7.

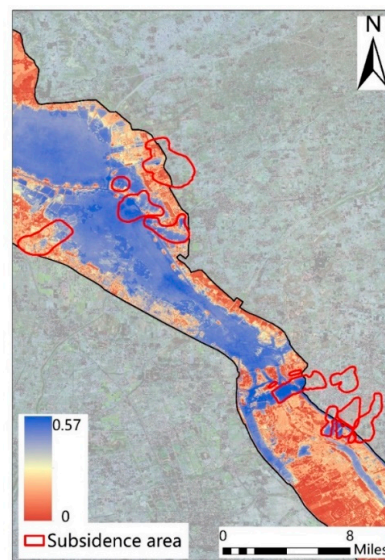


Figure 7. Distribution of subsidence area in Nansi Lake.

Considering the difference in the areas of subsidence and contrast areas, 100 and 1000 random points are selected to compare their values of SHP index, and one-way ANOVA is performed (Figure 8). Results show that the average SHP index in the subsidence area is 0.34 ± 0.12 , while the SHP index in the contrast area is 0.32 ± 0.1 , with no significant difference in SHP index between two areas at $p < 0.05$, which indicates that underwater mining has limited impact on the status, habitat, and potential of the plant communities.

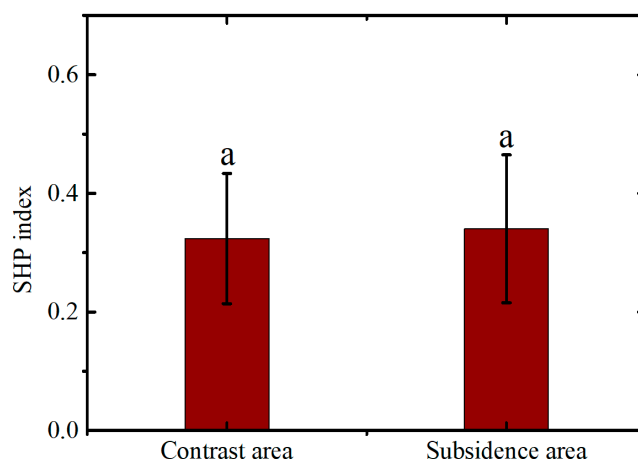


Figure 8. SHP indices in the subsidence and contrast areas of Nansi Lake. Different letters indicate significant differences between the SHP indices in the subsidence and contrast areas of Nansi Lake at $p < 0.05$ based on Duncan's multiple range test.

4. Discussion

4.1. Effects of Underwater Mining on Plant Communities in Wetland Ecosystems

Ground subsidence caused by underwater mining did not have significant impacts on plant communities. Ground subsidence has been considered as the main form of disturbance in underground mining areas, contributing to waterlogging and loss of plant communities [34–36]. However, it is worth noting that there are differences between the underwater mining areas and the lake caused by waterlogging, in terms of the changes in soil properties, species composition, and water properties. Waterlogging caused by mining subsidence would transform terrestrial ecosystems into wetland ecosystems, resulting in a complete change for original plant communities, while underwater mining mainly leads to fluctuations in the soil properties, species composition, and water level of subsidence areas. Therefore, it is necessary to distinguish the effects of subsidence induced by underground and underwater plant communities. In this study, significant differences were not found by comparing the SHP index between the subsidence and contrast areas, indicating that plant communities did not undergo dramatic changes in the subsidence areas. This may be due to the following reasons: (1) The offset of positive and negative effects of mining subsidence. Firstly, subsidence will alter the topography of the lake bottom, increase water depth, and influence soil properties, which could limit the growth of some emergent and submerged plants. Some terrestrial plants could also sink into the water and die (as shown in Figure 9a). New wetlands will appear in the subsidence areas with low depth (As shown in Figure 9b), thus recovering the number of wetland plant communities. Therefore, the positive and negative effects of underwater mining could enable plant communities in the subsidence areas stable on the whole. (2) The resilience of plant communities. Plant individuals and communities both have the ability to resist external interferences to a certain extent, that is, resilience [37], which allows vegetation to maintain structural and functional stability after subsidence and can recover within a certain threshold. Based on the above two reasons, the plant community in the subsidence area may not be severely affected by underwater mining within a certain time scale.

However, human activities accompanying coal mining under the lake may have a greater impact on wetland plant communities. According to the distribution of the SHP index, it can be found that river courses, lake shores, and estuaries, are areas with low SHP, which is largely due to the influence of human activities. Underground mining areas are generally accompanied by various human activities, such as agricultural planting, aquaculture, and coal washing, while coal mining under lakes has more diverse types of human activities. In the underwater mining area, it is easier to form water accumulation areas after subsidence, especially around the lake shore. Since villagers along the lake

have been engaged in fish farming for a long time, these areas are often transformed into fish ponds. Therefore, the plant communities in these areas and their surrounding areas are often transformed into fish ponds, leading to human control of the water body (as shown in Figure 10a). A large number of shipping vessels transporting coal is also widely distributed and will cause damage to the plant communities around the river, as well as to the plant communities at the bottom of the river (as shown in Figure 10b). Moreover, the damage caused by subsidence (shown in Figure 10c) will force residents to move to live around the lake (shown in Figure 10d), and the resulting discharge of domestic sewage may lead to water pollution and eutrophication, which will cause severe impacts on the local plant communities [38]. Furthermore, coal mining under lakes in some areas will also have a drastic impact on the regional hydrological system. Subsidence and cracks are likely to result in the destruction of underground aquifers, which may cause the loss of groundwater and the depletion of surface water, causing the original wetland ecosystem to transform into a terrestrial ecosystem. On the other hand, due to the developed water system in the coal mining area under the lake, there is often a closer connection between surface water, groundwater, and mine water, and the resulting water pollution problems (such as polycyclic aromatic hydrocarbons [39,40]) are also significantly more than those of other types. In general, the subsidence caused by coal mining under the lake has both positive and negative effects on the plant community. Overall, plant communities in subsidence areas may not be significantly different from those in surrounding areas, but various coal-related human activities will have a significant impact on plant communities.

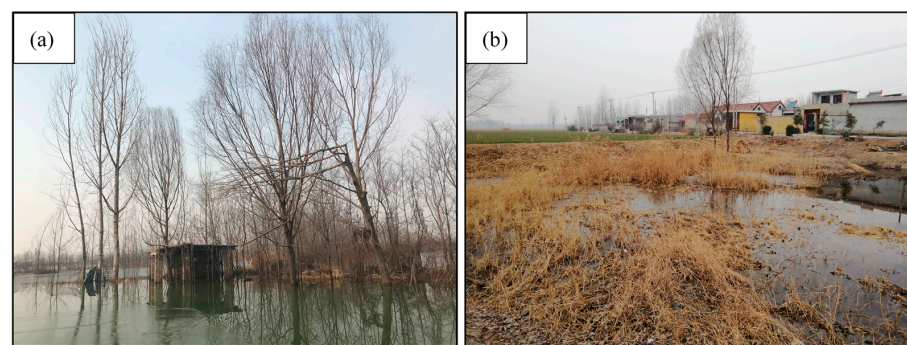


Figure 9. Effects of mining-induced subsidence with (a) high and (b) low depth on plant communities.



Figure 10. Human activities accompanied by underwater mining in Nansi Lake. (a) Fish ponds in the subsidence area, (b) coal shipping, (c) destruction of buildings in the subsidence area, and (d) settlements around the lake.

Differences in the temporal and spatial scales, as well as evaluation targets between the SHP model developed in this research and previous methods, could contribute to a diverse insight into the effect of underwater mining on plant communities. Most of the evaluation models for the plant community only focus on their status at a certain time point, and the statuses at different time points were compared directly to show the effects of disturbances. In the SHP model, the plant communities were evaluated from three different dimensions: status, habitat, and potential, which would lead to a different result compared with those methods considering status only in some cases. For example, some species in a community could be influenced by mining-induced subsidence and extinct, and the status of the plant community will decline in the short term. However, the habitat and potential of this community could remain stable, because other plant species are likely to substitute and survive after subsidence, indicating that the status of this plant community could recover. Therefore, the plant community in the above case could be considered less impacted according to the evaluation result in the SHP model than in other methods. From the perspectives of the temporal–spatial scale, the SHP model applies time series remote sensing images to evaluate plant communities for long time scales while considering the annual development of plant communities, driven by natural force, which not only eliminates the annual deviance between different months, but also the interannual deviance between various years, and thus, the evaluation results from SHP model could be more accurate than those methods using images at single time points. In terms of the spatial scale, the SHP model focuses on the overall conditions of plant communities within the pixel range of remote sensing images, which would inevitably ignore some changes in small scales, such as the death of one plant and the fluctuation of a community, showing a different evaluation result when compared with that in small scale research. Overall, based on the temporal and spatial scales, as well as evaluation targets of the SHP model, underwater mining could have a relatively small effect on plant communities.

4.2. Spatial Characteristics of Plant Communities in Underwater Mining Areas and Strategies for Protection

Under the multiple effects of underwater mining and accompanying human activities, lake shores, and river channels become areas with the most obvious fluctuations in plant communities. According to the results of the hot spot analysis and the Global Moran index, it can be found that there is an aggregated pattern in the plant communities of the Nansi Lake mining area. Hot spots and cold spots are concentrated in the center of the lake and the living area, respectively, while the SHP index in other areas shows a random distribution, especially on lake shores and river channels. As shown above, lakeshores and rivers are areas with intensive human activities in this region, including coal shipping, aquaculture, irrigation, and other activities, while these areas are also areas where water and land interact, which is generally believed to have the highest vegetation diversity. But relatively, these areas are also the most sensitive to changes in climate factors, especially water level fluctuations caused by inter-annual rainfall differences. Changes in water levels will not provide a stable habitat for plant communities, thus limiting the succession, and making it unsuitable for the emergence as well as growth of many perennial plants. Therefore, under the multiple effects of climate fluctuations and human activities, lake shores and river channels are the main areas where plant communities in underwater mining areas are damaged.

According to the spatial characteristics of plant communities and human activities in underwater mining areas, targeted strategies for ecological protection and restoration need to be carried out. (1) Identifying the primary disturbances in underwater mining areas. It is commonly believed that subsidence was the most dramatic disturbance in underground mining areas, while the results of the evaluation in the Nansi Lake mining area provide a novel finding, indicating diverse effects of mining activities under different geological environments and land covers. Therefore, as for underwater mining areas, a systematic evaluation should be performed to identify the primary disturbances for

ecological conservation and management in the study area. (2) Delineating reasonably the mining scope based on surface coverage types. According to the general rules of mining-induced subsidence, the depth of subsidence increases with the recommendation of the coal mining working face, until reaching the regional maximum subsidence value at full mining or super-full mining scenarios. Therefore, the scope of the subsidence can be determined before implementation through subsidence prediction, which should be distributed on the deeper lakes or river channels in the area, thereby avoiding or reducing damages to land, shoals, and lakeside plant communities due to large-scale and long-depth subsidence. (3) Formulating a restoration plan based on the spatial characteristics of the subsidence and water-logging areas. The formed subsidence and water-logging areas can be restored to different forms according to their spatial location, subsidence depth, and landscape characteristics. For example, some water accumulation areas with a deeper subsidence depth and closer to the shore can be reclaimed into cropland by covering it with soil. Some waterlogged areas with deep subsidence and poor connectivity to the lake can be selectively transformed into aquaculture areas, while those waterlogged areas located on both sides of the lakeshore and closely connected with the lake can be planted with wetland vegetation, to maintain the dynamic balance of the total wetland plant community. (4) Formulating protection plans based on regional production and lifestyle. In the Nansi Lake mining area, coal shipping, coal washing, and aquaculture are the main human disturbances to the regional plant community compared to mining subsidence. It is necessary to delineate protection scopes for these human activities, such as clearing industrial facilities, aquaculture fences, and residential areas on both sides of the river to reduce human interference, and gradually eliminate these disturbances through industrial transformation and establishment of protected areas. Overall, mining has always been considered a strong human disturbance, and most of the strategies for ecological protection and restoration have been implemented around mining disturbance. However, the various human activities associated with underwater mining should be the first priority in the protection strategy, targeted actions should be carried out for these disturbances rather than for mining activities.

4.3. Potentials for Application of Time Series Images in the Evaluation of Plant Communities

The dynamic characteristics of plant growth and community succession cannot be evaluated through one single remote-sensing image at a single time point. As the most important ecological element in the terrestrial ecosystem, the plant is an intuitive reflection of regional ecological conditions [41]. Therefore, the evaluation of plant communities is widely applied in the planning, restoration, and management of ecosystems [42]. Although the application of remote sensing technology has greatly reduced the subjectivity and randomness of traditional field surveys, remote sensing images at a single time point still have certain limitations and cannot accurately reflect the dynamic change process of plant communities. First of all, there are certain differences in the structural parameters such as coverage, diversity, and biomass of plant communities in different years. The leaf area, water content, and chlorophyll content of plants also change within one year. Remote sensing images at a single time point can only reflect the status of the plant community at the time of investigation, which reduces the representativeness of the overall status of the regional plant community, and it is also difficult to reflect the dynamic change process of plant communities. Moreover, remote sensing images are easily affected by factors such as cloud cover, ice, and snow coverage, leading to enormous noise in the remote sensing data. At last, the complexity of factors involving changes in vegetation could also prevent acquiring a clear insight into the effects on plant communities. The succession of plant communities is under the combined effects of different factors, such as soil, climate, and human activities, showing natural seasonal cycles and fluctuations. Therefore, it would be hard to distinguish the specified effect of one factor from combined effects.

Time series remote sensing images have great potential in the evaluation of plant communities. With the increase in the categories and amount of open satellite remote sensing

image data, such as Landsat, Sentinel, and GF series of remote sensing satellites, and the improvement of spatial resolution, as well as the increasing maturity of remote sensing cloud platforms, such as GEE, time series remote sensing has been widely applied in the monitoring and evaluation of ecosystems [43–45]. In terms of evaluation for plant communities, time series remote sensing mainly has the following advantages: (1) Reflecting the multi-dimensional characteristics of vegetation. Time series remote sensing can obtain the average value of plant indicators and thereby can be more accurate in reflecting the average level of its status. In addition, it can reflect the growth trend of dynamic changes in plant communities based on the variance, slope, and entropy of different plant indicators. For instance, the normalized spectral entropy was used to quantify the resilience of plant communities [46]. (2) Reflecting the impact of different disturbances on plant communities. When revealing the impact of disturbances on plant communities, it has been common in the past to evaluate and compare the status of plant communities in different years. However, this kind of method ignores the long-term impacts of some disturbances, such as subsidence, drought, and decline of groundwater level, which will last for years or months. Thus, impacts on plant communities from long-term disturbances may last for several years as well, forcing the plant community to gradually degrade. However, the comparison of plant communities at different years can easily ignore the degradation of plant communities, which is often simply attributed to the changes in plant types. Therefore, it is necessary to restore the complete process of plant community changes through time series remote sensing. (3) Improving the robustness of evaluation results. By collecting all available remote sensing data in the study area, time series indicators can effectively avoid errors resulting from missing data. Combining time series remote sensing algorithms can also eliminate outliers caused by data noise, thereby improving the accuracy and objectivity of the evaluation results. All in all, compared with traditional single-time point remote sensing images, time series remote sensing images have been significantly improved in terms of data quality, information dimension, and scope of application, and are especially suitable for the evaluation of plant communities under long-term disturbances. However, it is also worthwhile that although the time series remote sensing images can picture a relatively complete changing process of plant communities, other factors involved in the development of plant communities are still difficult to distinguish, and targeted models should be developed based on different purposes.

5. Conclusions

This study put forward a “Status-Habitat-Potential” model to evaluate the plant communities in underwater mining areas, with nine indicators from the status, habitat, and potentials of plant communities, and the plant communities in the Nansi Lake mining area evaluated. The results show that the SHP index in Nansi Lake varies between 0 and 0.57, and shows a high aggregation pattern according to Global Moran’s index (0.41), with high and low values of SHP index aggregating in the center of the lake and living areas, respectively, based on hot spot analysis. By comparing the values of the SHP index between subsidence and contrast areas, the plant communities are not significantly influenced by subsidence resulting from underwater mining. However, human activities accompanying underwater mining, such as coal shipping, aquaculture, and domestic wastewater, are the main disturbances in underwater mining areas, which limit the development of plant communities in the wetland ecosystem, especially for those around lake shores and river channels. The evaluation model developed in this study provides an approach to comprehensively reveal the status, habitat, and potential of plant communities in wetland ecosystems, and the effects of underwater mining on plant communities are illustrated, as well as strategies for protection in underwater mining areas, put forward based on spatial characteristics of plant communities under mining effects, which can provide a reference for ecological conservation and management in similar mining areas.

Supplementary Materials: The following supporting information can be downloaded at: <https://www.mdpi.com/article/10.3390/land12122097/s1>. Supplementary Materials S1 and S2: Code for images collection and adding NDVI and NDWI band on GEE.

Author Contributions: Conceptualization, J.M. and D.Y.; writing—original draft preparation, J.M. and D.Y.; writing—review and editing, J.M. and D.Y.; supervision, H.H. and S.Z.; funding acquisition, J.M. All authors have read and agreed to the published version of the manuscript.

Funding: This research was funded by the National Natural Science Foundation of China, grant number 52304194 and 52374175.

Data Availability Statement: The data presented in this study are available on request from the corresponding author.

Conflicts of Interest: The authors declare no conflict of interest.

References

- Bruno Rocha Martins, W.; Douglas Roque Lima, M.; de Oliveira Barros Junior, U.; Amorim, L.S.V.-B.; de Assis Oliveira, F.; Schwartz, G. Ecological methods and indicators for recovering and monitoring ecosystems after mining: A global literature review. *Ecol. Eng.* **2020**, *145*, 105707. [\[CrossRef\]](#)
- Mi, J.; Yang, Y.; Hou, H.; Zhang, S.; Ding, Z.; Hua, Y. Impacts of Ground Fissures on Soil Properties in an Underground Mining Area on the Loess Plateau, China. *Land* **2022**, *11*, 162. [\[CrossRef\]](#)
- Mi, J.; Liu, R.; Zhang, S.; Hou, H.; Yang, Y.; Chen, F.; Zhang, L. Vegetation patterns on a landslide after five years of natural restoration in the Loess Plateau mining area in China. *Ecol. Eng.* **2019**, *136*, 46–54. [\[CrossRef\]](#)
- Yang, D.; Qiu, H.; Ma, S.; Liu, Z.; Du, C.; Zhu, Y.; Cao, M. Slow surface subsidence and its impact on shallow loess landslides in a coal mining area. *Catena* **2022**, *209*, 105830. [\[CrossRef\]](#)
- Bi, Y.; Zhang, J.; Song, Z.; Wang, Z.; Qiu, L.; Hu, J.; Gong, Y. Arbuscular mycorrhizal fungi alleviate root damage stress induced by simulated coal mining subsidence ground fissures. *Sci. Total Environ.* **2019**, *652*, 398–405. [\[CrossRef\]](#)
- Mi, J.; Hou, H.; Zhang, S.; Hua, Y.; Yang, Y.; Zhu, Y.; Ding, Z. Detecting long-term effects of mining-induced ground deformation on plant succession in semi-arid areas using a cellular automata model. *Ecol. Indic.* **2023**, *151*, 110290. [\[CrossRef\]](#)
- Sun, X.; Yuan, L.; Liu, M.; Liang, S.; Li, D.; Liu, L. Quantitative estimation for the impact of mining activities on vegetation phenology and identifying its controlling factors from Sentinel-2 time series. *Int. J. Appl. Earth Obs. Geoinf.* **2022**, *111*, 102814. [\[CrossRef\]](#)
- Dolný, A.; Harabiš, F. Underground mining can contribute to freshwater biodiversity conservation: Allogenic succession forms suitable habitats for dragonflies. *Biol. Conserv.* **2012**, *145*, 109–117. [\[CrossRef\]](#)
- Pierzchala, L.; Sierka, E. Do submerged plants improve the water quality in mining subsidence reservoirs? *Appl. Ecol. Environ. Res.* **2020**, *18*, 5661–5672. [\[CrossRef\]](#)
- Ciszewski, D.; Sobucki, M. River response to mining-induced subsidence. *Catena* **2022**, *214*, 106303. [\[CrossRef\]](#)
- Antwi, E.K.; Krawczynski, R.; Wiegand, G. Detecting the effect of disturbance on habitat diversity and land cover change in a post-mining area using GIS. *Landsc. Urban Plan.* **2008**, *87*, 22–32. [\[CrossRef\]](#)
- Hou, H.; Ding, Z.; Zhang, S.; Chen, Z.; Wang, X.; Sun, A.; An, S.; Xiong, J. Targeting the Influences of Under-Lake Coal Mining Based on the Value of Wetland Ecosystem Services: What and How? *Land* **2022**, *11*, 2166. [\[CrossRef\]](#)
- Casanova, M.T.; Brock, M.A. How do depth, duration and frequency of flooding influence the establishment of wetland plant communities? *Plant Ecol.* **2000**, *147*, 237–250. [\[CrossRef\]](#)
- Dong, B.; Qin, B.; Gao, G.; Cai, X. Submerged macrophyte communities and the controlling factors in large, shallow Lake Taihu (China): Sediment distribution and water depth. *J. Great Lakes Res.* **2014**, *40*, 646–655. [\[CrossRef\]](#)
- Stoof-Leichsenring, K.R.; Dulias, K.; Biskaborn, B.K.; Pstryakova, L.A.; Herzsuh, U. Lake-depth related pattern of genetic and morphological diatom diversity in boreal Lake Bolshoe Toko, Eastern Siberia. *PLoS ONE* **2020**, *15*, e0230284. [\[CrossRef\]](#)
- Xiao, W.; Zheng, W.; Zhao, Y.; Chen, J.; Hu, Z. Examining the relationship between coal mining subsidence and crop failure in plains with a high underground water table. *J. Soils Sediments* **2021**, *21*, 2908–2921. [\[CrossRef\]](#)
- Guzy, A.; Malinowska, A.A. Assessment of the Impact of the Spatial Extent of Land Subsidence and Aquifer System Drainage Induced by Underground Mining. *Sustainability* **2020**, *12*, 7871. [\[CrossRef\]](#)
- Ma, L.; Jin, Z.; Liang, J.; Sun, H.; Zhang, D.; Li, P. Simulation of water resource loss in short-distance coal seams disturbed by repeated mining. *Environ. Earth Sci.* **2015**, *74*, 5653–5662. [\[CrossRef\]](#)
- Salimi, S.; Almuktar, S.A.; Scholz, M. Impact of climate change on wetland ecosystems: A critical review of experimental wetlands. *J. Environ. Manag.* **2021**, *286*, 112160. [\[CrossRef\]](#)
- Cao, B.; Bai, C.; Xue, Y.; Yang, J.; Gao, P.; Liang, H.; Zhang, L.; Che, L.; Wang, J.; Xu, J.; et al. Wetlands rise and fall: Six endangered wetland species showed different patterns of habitat shift under future climate change. *Sci. Total Environ.* **2020**, *731*, 138518. [\[CrossRef\]](#)
- Liu, Q.; Liu, J.; Liu, H.; Liang, L.; Cai, Y.; Wang, X.; Li, C. Vegetation dynamics under water-level fluctuations: Implications for wetland restoration. *J. Hydrol.* **2020**, *581*, 124418. [\[CrossRef\]](#)

22. Li, Y.; Qian, F.; Silbernagel, J.; Larson, H. Community structure, abundance variation and population trends of waterbirds in relation to water level fluctuation in Poyang Lake. *J. Great Lakes Res.* **2019**, *45*, 976–985. [[CrossRef](#)]
23. Hiatt, M.; Snedden, G.; Day, J.W.; Rohli, R.V.; Nyman, J.A.; Lane, R.; Sharp, L.A. Drivers and impacts of water level fluctuations in the Mississippi River delta: Implications for delta restoration. *Estuar. Coast. Shelf Sci.* **2019**, *224*, 117–137. [[CrossRef](#)]
24. Mu, S.; Li, B.; Yao, J.; Yang, G.; Wan, R.; Xu, X. Monitoring the spatio-temporal dynamics of the wetland vegetation in Poyang Lake by Landsat and MODIS observations. *Sci. Total Environ.* **2020**, *725*, 138096. [[CrossRef](#)] [[PubMed](#)]
25. Wei, G.-W.; Chen, Y.; Sun, X.-S.; Chen, Y.-H.; Luo, F.-L.; Yu, F.-H. Growth responses of eight wetland species to water level fluctuation with different ranges and frequencies. *PLoS ONE* **2019**, *14*, e0220231. [[CrossRef](#)] [[PubMed](#)]
26. Yin, D.; Peng, F.; He, T.; Xu, Y.; Wang, Y. Ecological risks of heavy metals as influenced by water-level fluctuations in a polluted plateau wetland, southwest China. *Sci. Total Environ.* **2020**, *742*, 140319. [[CrossRef](#)]
27. Tajduś, K.; Sroka, A.; Misa, R.; Hager, S.; Rusek, J.; Dudek, M.; Wollnik, F. Analysis of Mining-Induced Delayed Surface Subsidence. *Minerals* **2021**, *11*, 1187. [[CrossRef](#)]
28. Chang, C.C.; Turner, B.L. Ecological succession in a changing world. *J. Ecol.* **2019**, *107*, 503–509. [[CrossRef](#)]
29. Vorovencii, I. Changes detected in the extent of surface mining and reclamation using multitemporal Landsat imagery: A case study of Jiu Valley, Romania. *Environ. Monit. Assess.* **2021**, *193*, 30. [[CrossRef](#)]
30. Zhang, M.; Wang, J.; Li, S. Tempo-spatial changes and main anthropogenic influence factors of vegetation fractional coverage in a large-scale opencast coal mine area from 1992 to 2015. *J. Clean. Prod.* **2019**, *232*, 940–952. [[CrossRef](#)]
31. Huang, Y.; Tian, F.; Wang, Y.; Wang, M.; Hu, Z. Effect of coal mining on vegetation disturbance and associated carbon loss. *Environ. Earth Sci.* **2015**, *73*, 2329–2342. [[CrossRef](#)]
32. Lee, J.; Li, S. Extending Moran’s Index for Measuring Spatiotemporal Clustering of Geographic Events. *Geogr. Anal.* **2017**, *49*, 36–57. [[CrossRef](#)]
33. Wulff, A.S.; Hollingsworth, P.M.; Ahrends, A.; Jaffré, T.; Veillon, J.-M.; L’huillier, L.; Fogliani, B. Conservation Priorities in a Biodiversity Hotspot: Analysis of Narrow Endemic Plant Species in New Caledonia. *PLoS ONE* **2013**, *8*, e73371. [[CrossRef](#)] [[PubMed](#)]
34. Mi, J.; Yang, Y.; Hou, H.; Zhang, S.; Raval, S.; Chen, Z.; Hua, Y. The long-term effects of underground mining on the growth of tree, shrub, and herb communities in arid and semiarid areas in China. *Land Degrad. Dev.* **2021**, *32*, 1412–1425. [[CrossRef](#)]
35. Liu, S.; Li, W.; Qiao, W.; Wang, Q.; Hu, Y.; Wang, Z. Effect of natural conditions and mining activities on vegetation variations in arid and semiarid mining regions. *Ecol. Indic.* **2019**, *103*, 331–345. [[CrossRef](#)]
36. Yang, Z.; Li, W.; Li, X.; He, J. Quantitative analysis of the relationship between vegetation and groundwater buried depth: A case study of a coal mine district in Western China. *Ecol. Indic.* **2019**, *102*, 770–782. [[CrossRef](#)]
37. Speed, J.D.; Cooper, E.J.; Jónsdóttir, I.S.; Van Der Wal, R.; Woodin, S.J. Plant community properties predict vegetation resilience to herbivore disturbance in the Arctic. *J. Ecol.* **2010**, *98*, 1002–1013. [[CrossRef](#)]
38. Qin, B.; Gao, G.; Zhu, G.; Zhang, Y.L.; Song, Y.Z.; Tang, X.M.; Xu, H.; Deng, J.M. Lake eutrophication and its ecosystem response. *Chin. Sci. Bull.* **2013**, *58*, 961–970. [[CrossRef](#)]
39. Seopela, M.P.; McCrindle, R.I.; Combrinck, S.; Regnier, T.J.-C. Hazard assessment of polycyclic aromatic hydrocarbons in water and sediment in the vicinity of coalmines. *J. Soils Sediments* **2016**, *16*, 2740–2752. [[CrossRef](#)]
40. Chen, D.; Feng, Q.; Liang, H.; Gao, B.; Alam, E. Distribution characteristics and ecological risk assessment of polycyclic aromatic hydrocarbons (PAHs) in underground coal mining environment of Xuzhou. *Hum. Ecol. Risk Assess. Int. J.* **2019**, *25*, 1564–1578. [[CrossRef](#)]
41. Sitch, S.; Smith, B.; Prentice, I.C.; Arneth, A.; Bondeau, A.; Cramer, W.; Kaplan, J.O.; Levis, S.; Lucht, W.; Sykes, M.T.; et al. Evaluation of ecosystem dynamics, plant geography and terrestrial carbon cycling in the LPJ dynamic global vegetation model. *Glob. Chang. Biol.* **2003**, *9*, 161–185. [[CrossRef](#)]
42. Villoslada, M.; Bergamo, T.F.; Ward, R.D.; Burnside, N.; Joyce, C.; Bunce, R.; Sepp, K. Fine scale plant community assessment in coastal meadows using UAV based multispectral data. *Ecol. Indic.* **2020**, *111*, 105979. [[CrossRef](#)]
43. Lee, C.K.; Nicholson, E.; Duncan, C.; Murray, N.J. Estimating changes and trends in ecosystem extent with dense time-series satellite remote sensing. *Conserv. Biol.* **2021**, *35*, 325–335. [[CrossRef](#)] [[PubMed](#)]
44. Xu, H.; Wang, Y.; Guan, H.; Shi, T.; Hu, X. Detecting Ecological Changes with a Remote Sensing Based Ecological Index (RSEI) Produced Time Series and Change Vector Analysis. *Remote Sens.* **2019**, *11*, 2345. [[CrossRef](#)]
45. Sandeep, P.; Obi Reddy, G.P.; Jegankumar, R.; Kumar, K.A. Monitoring of agricultural drought in semi-arid ecosystem of Peninsular India through indices derived from time-series CHIRPS and MODIS datasets. *Ecol. Indic.* **2021**, *121*, 107033. [[CrossRef](#)]
46. De Keersmaecker, W.; Lhermitte, S.; Honnay, O.; Farifteh, J.; Somers, B.; Coppin, P. How to measure ecosystem stability? An evaluation of the reliability of stability metrics based on remote sensing time series across the major global ecosystems. *Glob. Chang. Biol.* **2014**, *20*, 2149–2161. [[CrossRef](#)]

Disclaimer/Publisher’s Note: The statements, opinions and data contained in all publications are solely those of the individual author(s) and contributor(s) and not of MDPI and/or the editor(s). MDPI and/or the editor(s) disclaim responsibility for any injury to people or property resulting from any ideas, methods, instructions or products referred to in the content.